Chinese Chemical Letters 32 (2021) 3509–3513

Contents lists available at ScienceDirect

Chinese Chemical Letters

journal homepage: www.elsevier.com/locate/cclet

Communication

Preparation of quaternarized *N*-halamine-grafted graphene oxide nanocomposites and synergetic antibacterial properties

Danlin Bu[a,b], Yu Zhou[a,b], Chang Yang[a,b], Hengyu Feng[a,b], Chunxia Cheng[a,b], Mengjie Zhang[a], Zice Xu[a], Linghan Xiao[a,b,**], Yujing Liu[c,*], Zhenai Jin[d,*]

[a] *Jilin Province Key Laboratory of Carbon Fiber Development and Application, College of Chemistry and Life Science, Changchun University of Technology, Changchun 130012, China*
[b] *Advanced Institute of Materials Science, Changchun University of Technology, Changchun 130012, China*
[c] *College of Materials Science and Engineering, Zhejiang University of Technology, Hangzhou 310014, China*
[d] *Department of Pediatrics, Affiliated Hospital of Yanbian University, Yanji 133000, China*

ARTICLE INFO

Article history:
Received 17 January 2021
Received in revised form 17 February 2021
Accepted 2 March 2021
Available online 4 March 2021

Keywords:
N-Halamine
Quaternary ammonia salt
Graphene oxide
Synergetic sterilization
Nanocomposite

ABSTRACT

At present, frequent outbreaks of bacteria and viruses have seriously affected people's normal lives. Therefore, the study of broad-spectrum antibacterial nanocomposites is very promising. However, most antibacterial materials have some disadvantages, such as single bactericidal mechanisms and unrepeatable use. Based on the current situation, a kind of nanocomposite with three structures of graphene oxide (GO), quaternary ammonium salt (QAs) and *N*-halamine was prepared, which showed synergistic effect to improve antibacterial activity and combined with a variety of sterilization mechanisms. Meanwhile, GO can provide richer ways of sterilization and high specific surface area, which is conducive to the grafting of quaternarized *N*-halamine. The advantages of physical sterilization of GO, charge adsorption of QAs, reuse of *N*-halamine and efficient sterilization are fully utilized. The results showed that the quaternarized *N*-halamine-grafted GO was obtained successfully. GO grafted with quaternarized *N*-halamine polymer showed strong speedy bactericidal activity against *Escherichia coli* (*E. coli*) *and Staphylococcus aureus* (*S. aureus*) (99%). It had good storage and regeneration properties.

As bacteria and viruses threaten people's health and life all the time, the development and research of various antibacterial materials have been going on for many years [1]. Through the continuous efforts of researchers, a variety of antimicrobial agents have emerged such as free halogen [2], metal oxide [3], quaternary ammonium salt (QAs) [4], peptide [5], guanidine and *N*-halamines [6], graphene oxide (GO) is also one of them. However, the antibacterial mechanism of an antimicrobial agent is generally single [7]. Although GO has been found to have a variety of bactericidal mechanisms, such as oxidative stress, physical/mechanical damage, photothermal/photocatalytic effect [8], inhibition of bacterial metabolism, lipid extraction and isolation by wrapping [9]. Its bactericidal efficacy still needs to be improved [10]. The compound use of a variety of antimicrobial agents to obtain stronger germicidal efficacy has become an important way to prepare high-efficiency antibacterial materials [11]. In recent years, GO has been widely used in the fields of antibacterial action [12], bio detection [13], cancer treatment [14], drug [15] and gene delivery [16] because of its unique physical and chemical properties, such as wide surface area, excellent electrical conductivity, thermal conductivity and bio-compatibility [17]. *N*-Halamine has also become a concerned antimicrobial agent because of its unique high biocidal efficacy and recharge ability. Because of its oxidizing properties, halogens in the N—X (X = Cl, Br, I) bond could provide high bactericidal activity by releasing bactericidal ions [18]. As soon as the halogen is released from the N—X bond, it can be charged by rehalogenation again [19]. Yang et al. found GO loaded with cuprous oxide nanoparticles, which was long-term antibacterial stable [3]. The antibacterial effect of these composites is much higher than that of single GO or single component, and has a synergistic bactericidal mechanism. Quaternarized *N*-halamines were synthesized by combining QAs with *N*-halamines, which can improve the bactericidal properties of materials by synergies of contact sterilization and release sterilization [20]. QAs is also a widely used antimicrobial agent

* Corresponding authors.
** Corresponding author at: Jilin Province Key Laboratory of Carbon Fiber Development and Application, College of Chemistry and Life Science, Changchun University of Technology, Changchun 130012, China.
E-mail addresses: xiaolinghan1981@163.com (L. Xiao), yujingliu@zjut.edu.cn (Y. Liu), 15526770675@163.com (Z. Jin).

https://doi.org/10.1016/j.cclet.2021.03.007
1001-8417/

with high positive charge. It can strongly attract the negatively charged bacteria on the surface, change the permeability of the cell membrane [21], and make the outflow of cell contents, which leads to contact killing. It is expected to design a multi-way synergistic sterilization of quaternarized *N*-halamine-grafted GO. For the purpose of realizing the above hypothesis, quaternarized *N*-halamine was grafted on GO to enrich the bactericidal pathway and improve the bactericidal efficacy. Using GO nanosheets as polymer back bones, poly(4-vinylpyridine) (P-4VP) grafted GO was synthesized by *in-situ* radical polymerization (ISRP). Large specific surface area provided more reaction sites and then 3-bromopropyl-5-5-dimethylhydantoin (BHD) was grafted by quaternization reaction to complete the preparation of quaternarized *N*-halamine grafted GO as shown in Scheme 1. In this contribution, combining with "release-kill" and "contact-kill" methods, the bactericidal efficacy of the material on *Escherichia coli* (*E. coli*) *and Staphylococcus aureus* (*S. aureus*) represented by Gram-negative and Gram-positive bacteria was studied. The synergistic effect was further investigated.

Fourier transform infrared spectroscopy (FT-IR) spectra of GO, 4-vinylpyridine-modified graphene oxide (GO-VP), *N*-halamine-immobilized GO-VP (GO-VPBHD) and quaternarized *N*-halamine-modified GO after chlorination treatment (GO-VPHD-Cl) are presented in Fig. 1. The FT-IR spectra of GO-VP showed bands at 1600, 1467 and 1415 cm^{-1} which were assigned to C=N and C=C stretching vibrations in pyridine group in Fig. 1a, respectively [22]. This illuminates that P-4VP was grafted on the GO. By contrast, new peaks at 1695 cm^{-1} of GO-VPBHD appeared because of the amide group (—CO—NH—) [23]. The success of *N*-quaternarized was verified by the C=N^+ stretching band at 1639 cm^{-1}. After chlorination treatment, the stretching vibration peak shifted from 1695 cm^{-1} to 1702 cm^{-1}, which was due to the electron withdrawing effect of oxidative chlorine [24]. Therefore, the FT-IR results showed that VPBHD had been grafted onto GO, and QAS was formed after the successful grafting of BHD.

The thermal stability of the samples was studied by thermogravimetric analysis (TGA). Fig. S1 showed the TGA of GO and the functionalized samples in supporting information. It was observed that the weight loss of the original GO occurred slightly in the range of ambient temperature to 120 °C, which was thermally unstable. This might be due to the removal of water adsorbed by oxygen-containing functional groups on the GO surface [25]. The main weight loss range of GO was from 180 °C to 230 °C, and the maximum weight loss rate was about 210 °C. This provided a good control for the follow-up samples. In contrast, different from the original GO nanowires, GO-VP exhibited a major mass loss between 300 °C and 400 °C, and the maximum weight loss rate was about 360 °C. After P4-VP modification, the weight loss of the material decreased obviously at about 210 °C, which may be attributed to the chemical bond interaction between P-4VP and GO

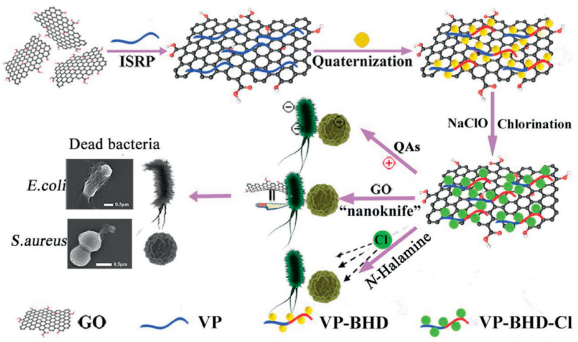

Scheme 1. Schematic illustration of the preparation of quaternarized *N*-halamine-grafted GO nanocomposites and the corresponding antibacterial mechanism.

matrix. At the same time, P-4VP has a higher decomposition temperature, which improved the thermal stability of the material [26]. The decomposition temperature (T_{max}, 322 °C) of GO-VPBHD-Cl was lower than that of unchlorinated GO-VPBHD (T_{max}, 330 °C).

The full scan X-ray photoelectron spectroscopy (XPS) of the GO, GO-VP, GO-VPBHD and GO-VPBHD-Cl were analyzed to mensurate the chemical comprise and chemical binding state of the sample (Fig. 1). The main elements on the surface were carbon and oxygen, which belonged to the oxygen-original GO containing groups on the base and edge of GO and their sp2-bonded carbon atoms, and the binding energy of the GO, GO-VP, GO-VPBHD and GO-VPBHD-Cl were analyzed by XPS to determine the chemical composition and chemical binding state of the sample (Fig. 1b). The main elements were on the 531.85 and 285.56 eV, respectively. After P-4VP modification, a peak appeared at binding energy of 400.85 eV, which corresponded to the N 1s in the pyridine polymeric. Therefore, P-4VP was favoringly grafted onto the surface of GO by *in-situ* polymerization. After quaternization by BHD, two new peaks of Br in GO-VPBHD appeared at binding energy of 181 and 66 eV, respectively. After chlorination, Cl 2p appeared at 200.8 eV because of the hydrogen in the *N*-halamine precursor was substituted by chlorine which also proved that of grafted VPBHD on GO occurred. For further identification, the deconvolutions of Br 3d, C 1s, N 1s and Cl 2p energy level were also performed, and the results were shown in Figs. 1c–f. The two peaks of 67 and 68 eV were caused by Br- in the ionic bond which formed by quaternization. For the GO-VPBHD-Cl, the C 1s peak was separated into six divided peaks such as —COOH, C=O, C—C and C—N/C—N^+ bonds. In the X-ray photoelectron spectroscopy of GO-VPBHD-Cl, there were three typical N 1s peaks at 399.9, 401.1 and 402.1 eV, respectively, pointing to the covalent bond imide nitrogen (—N<), amide nitrogen (>NCl) and C—N^+. The existence of these characteristic peaks indicated the chemical composition of GO grafted with quaternarized *N*-halamine (GO-VPBHD-Cl) [27]. After chlorination, the Cl 2p peak appeared obviously. This showed that chlorine was successfully loaded on the polymer during the chlorination process, which provided a strong evidence for the transition from N—H bond to N—Cl bond.

The surface morphologies of GO and its gradually modified samples were observed by scanning electron microscopy (SEM) in Fig. S3 (Supporting information). As shown in Fig. S3, GO can be clearly observed with a smooth surface and slight fold or crease on the edges. In contrast, the surface of the modified GO nanosheets was covered with P-4VP. Furthermore, the surface of GO-VPBHD was relatively glabrate and grayish white, which was ascribe to the decorating of DMH onto the surface of GO, while in Fig. S3d, the surface of chlorinated GO-VPBHD was rougher, which may be due to the etching of oxygenated chlorine [25].

The antibacterial kinetics of GO-VPBHD-Cl is the key factor which affects its application. The inactivation ability of GO-VPBHD, GO-VPBHD-Cl and the control group (bacterial suspension diluted with aseptic distilled water) was shown in Fig. 2, showing the survival of bacteria after exposure to control group, GO-VPBHD and GO-VPBHD-Cl for 10 min in Fig. 2a, respectively. The small spots on the culture plate represented bacterial colonies *S. aureus* (the first row of petri dishes) and *E. coli* (the second row of petri dishes). Until the action for 10 min, the killing rates of *E. coli* and *S. aureus* basically reached more than 99.9%. Excellent germicidal effect was achieved in a short time. The minimum inhibitory concentration (MIC) and minimum bactericidal concentration (MBC) were shown in Table. S1 (Supporting information). The results showed that the killing effect of GO-VPBHD-Cl with QAs structure and *N*-halamine structure on *E. coli* and *S. aureus* was better than that of GO-VPBHD with only QAs structure. Quaternarized *N*-halamine-grafted GO has good antibacterial effect. SEM was used to detect the morphological changes of selected bacteria after exposure to

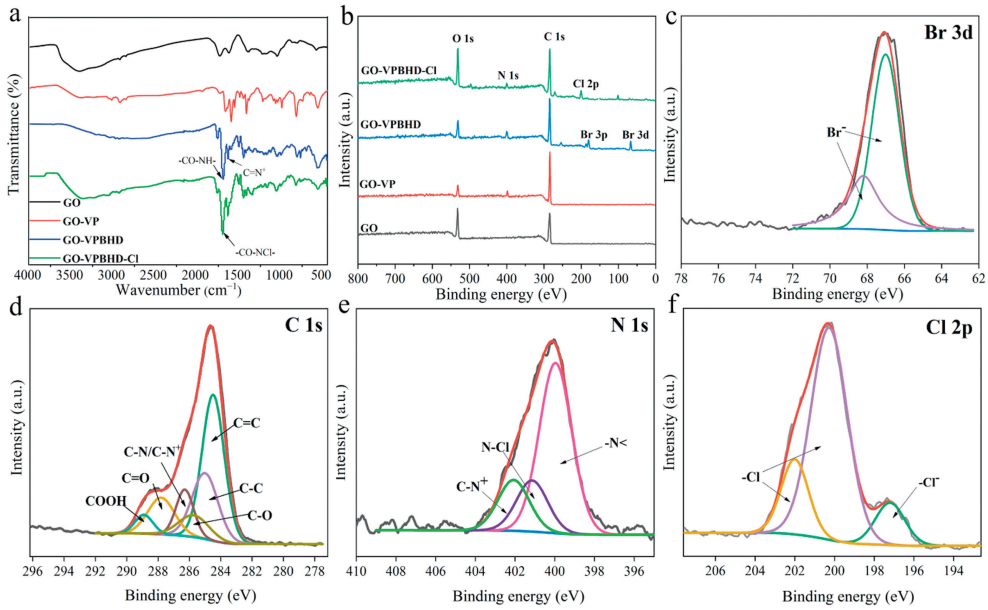

Fig. 1. (a, b) FT-IR spectra and XPS wide scan spectra of GO, GO-VP, GO-VPBHD and GO-VPHD-Cl, respectively. (c) Br 3d of GO-VPBHD, (d) C 1s of GO-VPBHD-Cl, (e) N 1s of GO-VPBHD-Cl, (f) Cl 2p of GO-VPBHD-C.

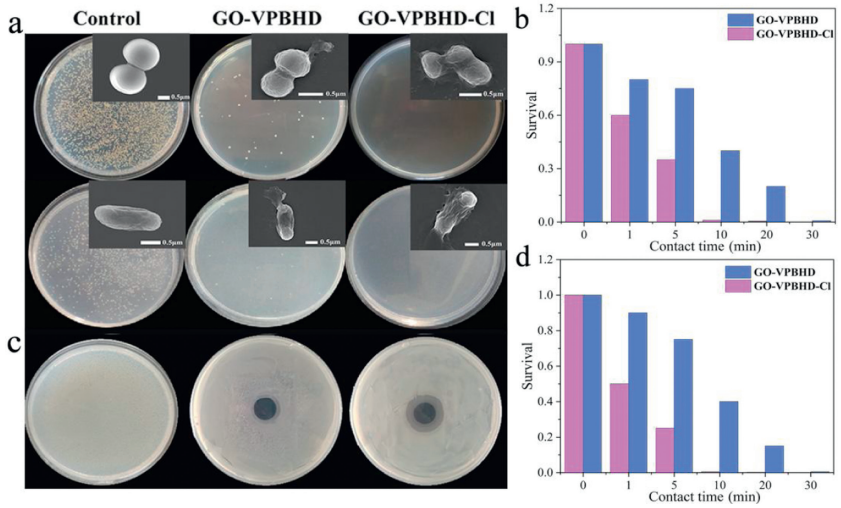

Fig. 2. Photographs of *S. aureus* (a) and *E. coli* (b) colonies grew upon a 10 min exposure to the samples (the inset shows the SEM images of bacterial cells). The results of the antibacterial kinetic tests for GO-VPBHD and GO-VPBHD-Cl against *S. aureus* (c) and *E. coli* (d) were shown.

GO-VPBHD and GO-VPBHD-Cl, as shown in the insertion section of Fig. 2a. After exposure to GO-VPBHD, *E. coli* and *S. aureus* lost their original intact structures with surface roughness and blistering. Similarly, the bacteria treated with GO-VPBHD-Cl also lost their original appearance with folds and rupture around the damaged outer membrane. Studies had shown that free chlorine can make GO into smaller slices [28], which also helped the quaternary ammonium *N*-halamine-modified GO display a blade/knife-like action to cause bacterial membrane destruction.

In addition, these results suggested that GO-VPBHD might kill bacteria by disrupting their surface charge balance and altering their membrane permeability. The GO-VPBHD-Cl sterilized efficiently by the release of chlorine ions. Similarly, the bacteria treated with GO-VPBHD-Cl also lost their original appearance with folds and rupture around the damaged outer membrane. Studies had shown that free chlorine can make GO into smaller slices [27], which also helped the quaternary ammonium *N*-halamine-modified GO display a blade/knife-like action to cause bacterial membrane destruction. In addition, these results suggested that GO-VPBHD might kill bacteria by disrupting their surface charge balance and altering their membrane permeability. The GO-VPBHD-Cl sterilized efficiently by the release of chlorine ions.

In order to further determine its killing mechanism, the bacteriostatic zone test was carried out with *E. coli* as the representative bacteria. It was acceptable that the bacteriostatic zone could not only reflect the sensitivity of bacteria to antimicrobial agents, but also reflect their antibacterial mechanism to a certain extent. As shown in Fig. 2b, the GO-VPBHD samples showed the inhibition ring around the sample disc. The results indicated that the QAs-containing GO-VPBHD kill bacteria by the positively charged ammonium group favor interaction with negatively charged bacterial cell membrane to disrupt membrane barrier function. Furthermore, a closer observation of the inhibition zone assay showed that the GO-VPBHD-Cl had a much

broader inhibition area than the GO-VPBHD. The results indicated that GO-VPBHD-Cl kill bacteria by some of the oxidative halogen diffused. So the release killing mechanism was also one possible way for the *N*-halamines to perform antibacterial function.

The results showed that the combination of QAs and *N*-halamine was more effective in killing bacteria. In order to verify their antibacterial effect, the antibacterial kinetic test was performed using both *E. coli* and *S. aureus.* Figs. 2c and d provided the corresponding results based on the calculated survival case as follows. The survival rate = (A/B) (where A is the number of surviving bacterial colonies of the test sample and B is that of the control). *S. aureus* was treated with the same concentration of GO-VPBHD and GO-VPBHD-Cl (Fig. 2c), and the bacterial survival rate was 0% after the treatment of 10 min. For the *E. coli* in Fig. 2d, both GO-VPBHD and GO-VPBHD-Cl inactivate about 99% of *E. coli* in 10 min. From these data, we can also find that the sterilization rate of GO materials modified with both *N*-halamine and QAs was faster than those with QAs, which is predictable. The most reasonable explanation is that the combination of the adsorption and antibacterial of QAs and the release and sterilization of *N*-halamine greatly improves the comprehensive antibacterial ability of the material. So that GO-VPBHD-Cl can kill *S. aureus* and *E. coli* in 10 min. The synergistic germicidal efficacy of the three is better than that of some materials with only QAs and *N*-halamine [29]. For example, our materials are faster in germicidal efficiency than TiO_2 nanotube-Ag-QAS [30], killing 99% of *E. coli* and *S. aureus* in 10 min of contact, and more efficient than GO with *N*-halamine in germicidal efficacy [24].

As shown in Fig. 3, oxide first oxidized iodine ions to form iodine (Fig. 3b). The antibacterial effect of *N*-halamine is based on the fact that oxidizing halogen to destroy or inhibit the metabolic process of microorganisms. Therefore, the antibacterial behavior of *N*-halamine must be related to the transformation of N—H/N—Cl. In addition to FTIR, XPS and other physical means, the modified GO was further verified by iodometry/thiosulfate titration. It was well known that iodometric/thiosulfate titration mainly involves two redox reactions, which shows color changes in the titration process. The prepared iodine could produce color reaction after adding starch solution, showing a blue suspension (Fig. 3c). Iodine could then be exhausted by titrated thiosulfate to fade (Fig. 3d). The change of color was not only the effective evidence of redox reaction, but also the evidence of the existence of *N*-halamine. Since the N—Cl structure would turn into N—H after killing bacteria, the recharging capacity of N—H and the stability of N—Cl structure were very important for practical antibacterial applications, so these properties of GO-VPBHD-Cl were studied as follows in Fig. 3e [31].

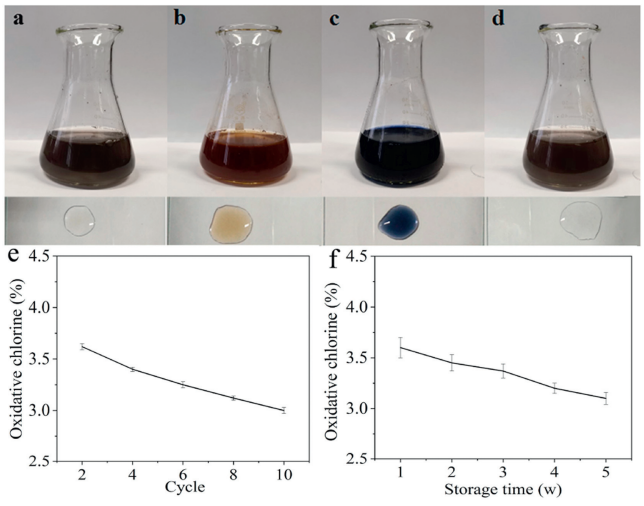

Fig. 3. (a)–(d) The color change involved in the iodometric/thiosulfate titration. (e) The oxidative chlorine content (Cl^+%) of GO-VPBHD-Cl during ten recycles. (f) The storage stability of GO-VPBHD-Cl.

For the rechargeable test of materials, GO-VPBHD-Cl was quenched with excessive sodium thiosulfate aqueous solution, so that the N-Cl structure was completely converted into N—H bond, and then chlorinated with NaClO aqueous solution, as described above. After 2, 4, 6, 8 and 10 cycles quenching chlorination, the mass percentage of chlorine decreased slightly from the initial 3.7 wt% to 3.62, 3.4, 3.25, 3.12 and 3 wt% in Fig. 3e, indicating that rechlorination had good recharging properties for the lost chlorine. Fig. 3f evaluated the retention and durability of chlorine oxide by storing GO-VPBHD-Cl in a condition box under laboratory illumination conditions (25 °C and 65% relative humidity) for 1, 2, 3, 4 and 5 weeks. After 5 weeks of storage, the chlorine content was only reduced by 16%, so the synthesized GO-VPBHD-Cl has good storage stability.

In this study, the quaternarized *N*-halamine-grafted GO (GO-VPBHD-Cl) was synthesized by covalently polymerizing VPBHD to the surface of GO. The fungicide based on the GO-VPBHD shows a high inactivation rate (>99.9%) against both Gram-negative *E. coli* and Gram-positive *S. aureus*. The combined use of GO, QAs and *N*-halamine made the material had efficient germicidal efficacy. The material makes full use of the advantages of cationic QAS site to attract bacteria, efficient contact sterilization of *N*-halamine, physical sterilization of GO and large specific surface area to achieve the synergistic effect of various germicidal mechanisms. The quaternarized *N*-halamine-grafted GO greatly manifested the superiority of multiple antibacterial mechanisms. The synthesis reaction solvent is water, and organic solvents are not used, which is more environmentally friendly. At the same time, the material has good cycle stability and storage stability, which lays a good foundation for its further preparation of coatings, gels, films and other composites, and has a broad application prospect.

Declaration of competing interest

The authors declare that they have no known competing financial interests or personal relationships that could have appeared to influence the work reported in this paper.

Acknowledgments

This work was supported by the National Natural Science Foundation of China (No. 51603020) and the Jilin Province Science and Technology Natural Science Foundation Project of China (No. 20180101193JC).

Appendix A. Supplementary data

Supplementary material related to this article can be found, in the online version, at doi:https://doi.org/10.1016/j.cclet.2021.03.007.

References

[1] J.M. Xia, W.J. Wang, X. Hai, et al., Chin. Chem. Lett. 30 (2019) 421–424.
[2] L. Li, W. Ma, X.L. Cheng, et al., Colloids Surf. B: Biointerfaces 148 (2016) 511–517.
[3] Z. Yang, X. Hao, S. Chen, et al., J. Colloid Interface Sci. 533 (2019) 13–23.
[4] D. He, Y. Yu, F. Liu, et al., Chem. Eng. J. 382 (2020) 122976.
[5] M. Kai, W. Zhang, H. Xie, et al., Chin. Chem. Lett. 29 (2018) 1163–1166.
[6] N. Porteous, J. Luo, M. Hererra, J. Schoolfield, Y. Sun, Int. J. Microbiol. 2011 (2011)767314.
[7] L. Xiao, X. Zheng, T. Zhao, et al., Colloid Polym. Sci. 291 (2013) 2359–2364.
[8] L.W. Han, J. Tan, J. Li, et al., Mol. Phys. 118 (2020) 1736674.
[9] Q. Xin, H. Shah, A. Nawaz, et al., Adv. Mater. 31 (2019) 1–15.
[10] S. Liu, T.H. Zeng, M. Hofmann, et al., ACS Nano 5 (2011) 6971–6980.

[11] T. Yang, N. Li, X.Y. Wang, et al., Chin. Chem. Lett. 31 (2020) 145–149.
[12] N. Pan, Y. Liu, X. Fan, et al., J. Mater. Sci. 52 (2016) 1996–2006.
[13] S.R. Joshi, A. Sharma, G.H. Kim, J. Jang, Mater. Sci. Eng. C 108 (2020) 110465.
[14] Y.F. Wang, G.P. Sun, Y.Y. Gong, et al., Nanoscale Res. Lett. 15 (2020) 57.
[15] Y.F. Wang, H.T. Zhang, J. Xie, et al., Colloids Surf. A: Physicochem. Eng. Aspects 590 (2020) 124498.
[16] H. Shen, H. Lin, A.X. Sun, et al., Acta Biomater. 105 (2020) 44–55.
[17] Y.J. Liu, K. He, W.T. Yuan, et al., Chin. Chem. Lett. 29 (2018) 1666–1670.
[18] A. Dong, Y.J. Wang, Y. Gao, T. Gao, G. Gao, Chem. Rev. 117 (2017) 4806–4862.
[19] F. Hui, C. Debiemme-Chouvy, Biomacromolecules 14 (2013) 585–601.
[20] Y. Liu, Y. Liu, X. Ren, T.S. Huang, Appl. Surf. Sci. 296 (2014) 231–236.
[21] H. Liu, X. Liu, F. Zhao, et al., J. Colloid Interface Sci. 562 (2020) 182–192.
[22] W. Cao, X. Peng, X. Chen, et al., J. Mater. Sci. 52 (2016) 1856–1867.
[23] M. Chylińska, H. Kaczmarek, A. Burkowska-But, Colloids Surf. B: Biointerfaces 176 (2019) 379–386.
[24] A. Dong, Q. Zhang, T. Wang, et al., J. Phys. Chem. C 114 (2010) 17298–17303.
[25] N. Pan, Y. Wang, X. Ren, T.S. Huang, I.S. Kim, Mater. Sci. Eng. C 103 (2019) 109877.
[26] S. Qin, D. Qin, W.T. Ford, J.E. Herrera, D.E. Resasco, Macromolecules 37 (2004) 9963–9967.
[27] Y. Chen, C. Feng, Q. Zhang, et al., Colloids Surf. B: Biointerfaces 187 (2020) 110642.
[28] S. An, J. Wu, Y. Nie, W. Li, J.D. Fortner, Chem. Eng. J. 381 (2020) 122609.
[29] R. Bai, Q. Zhang, L. Li, et al., ACS Appl. Mater. Interfaces 8 (2016) 31530–31540.
[30] X. Chen, K. Cai, J. Fang, et al., Surf. Coat. Technol. 216 (2013) 158–165.
[31] M. Zuo, N. Pan, T.S. Huang, I.S. Kim, X. Ren, Nano 15 (2020) 2050027.